Colloid Polym Sci 277:947–956 (1999)

ORIGINAL CONTRIBUTION

Y. Nagasoe
N. Ichiyanagi
H. Okabayashi
S. Nave
J. Eastoe
C.J. O'Connor

Raman scattering spectra of Aerosol-OT homologous sodium dialkylsulfosuccinates and the environment of their hydrophobic chains

Received: 23 February 1999
Accepted: 10 May 1999

Y. Nagasoe · N. Ichiyanagi
H. Okabayashi (✉)
Department of Applied Chemistry
Nagoya Institute of Technology
Gokiso-cho, Showa-ku
Nagoya 466-8555
Japan

S. Nave · J. Eastoe
School of Chemistry
University of Bristol, Cantock's Close
Bristol BS8 1TS, UK

C.J. O'Connor
Department of Chemistry
The University of Auckland
Private Bag 92019, Auckland 1
New Zealand

Abstract A homologous series of sodium dialkylsulfosuccinates (SDAS) has been synthesized with various chain lengths (dibutyl, dihexyl, diheptyl, dioctyl, dinonyl, didecyl, diundecyl and didodecyl). These compounds are straight-chain analogues for Aerosol-OT. Raman scattering spectra have been recordered for these SDAS compounds, both in the solid state and in aqueous solutions. These spectra are analyzed in detail in the CH stretch and CH_2 deformation regions, and the results depend specifically on the length of the hydrocarbon chain. In particular, the longitudinal accordion-like vibrational modes coming from the all-trans *n*-alkyl chains have been investigated. For the SDAS dihydrates, all hydrocarbon chains take up an extended form, whereas for the monohydrates the tails tend to become disordered at the CH_2-CH_2 single bond close to the terminal methyl groups. It has also been confirmed that for the concentrated aqueous SDAS (sodium dibutylsulfosuccinate – sodium dioctylsulfosuccinate) samples preferential stabilization of the extended conformation of the hydrocarbon chain may occur.

Key words Raman spectra · Sodium dialkylsulfosuccinates · Hydrophobic chains · Environment

Introduction

A number of vibrational studies of sodium bis(2-ethylhexyl)sulfosuccinate (Na-AOT) have been carried out both in the reverse micellar state and in microemulsions [1–15]. The vibrational spectra of Na-AOT consist mainly of the vibrational modes coming from the hydrophobic 2-ethylhexyl chains, the CH-CH_2 segment of the succinate skeleton, and the hydrophilic sulfonate and two ester portions. These modes in the 500–700, 1000–1300, and 1700–1750 cm^{-1} regions complicate the vibrational spectrum. Moreover, such a complex spectrum makes assignment of the bands very difficult. Most vibrational studies on AOT micellar and microemulsion systems have focused on the vibrational modes of water molecules incorporated into their microphases [2–8] and on those of the skeletal 2-ethylhexyl groups [9, 10].

Recently, Moran et al. [14] investigated the Fourier transform (FT)IR and FT-Raman spectra of various alkali-metal and tetraphenylarsonium salts of AOT and analyzed the vibrational modes associated with the head group of the AOT molecule [14]. Using vibrational spectroscopy, they also examined the structure of the AOT reverse micelles and water-in-oil microemulsions [15].

In the application of vibrational spectroscopy to model membrane systems, the relative intensity, I (2885 cm^{-1})/I (2850 cm^{-1}), of the bands in the CH stretch region has been widely referred to as a probe for studying the ordering and the environment of the hydrocarbon moiety [16–24]. Significant use of the CH stretch bands is still made to investigate the structure and environment of the hydrocarbon moiety in model membrane systems. Nevertheless, in the vibrational spectra of the Na-AOT molecule, the vibrational bands characteristic of CH_2 groups come from both the CH-CH_2 portion of the succinate skeleton and the two 2-ethylhexyl portions, although assignment of

the CH stretch bands to each portion has not yet been done.

In this present study, a series of sodium dialkylsulfosuccinates (SDAS), which are straight-chain analogues of Na-AOT, have been synthesized. The aim was to characterize the Raman scattering bands arising from the succinate CH-CH_2 portion and dialkyl chains. In particular, the CH-stretch and CH_2 deformation modes, as well as the accordion-like vibrational modes, are discussed in detail.

It has been possible to determine the effect of alkyl chain length on the vibrational spectra of these AOT analogues. This is helpful for understanding possible effects of chain length on crystalline, liquid crystalline, micellar, and microemulsion properties of these compounds. Studies of adsorption onto both air–water and oil–water interfaces are in hand, and the detailed information on molecular conformations described here may well be important for interpreting the significant effects of chemical structure.

Experimental

Materials

Sodium dimethylsulfosuccinate (SDMS) and sodium dideuteratedmethylsulfosuccinate (SDdMS) were synthesized as follows. Reactions of maleic acid anhydride with methyl alcohol or deuterated methyl alcohol were performed in dried benzene under reflux (328 K) for 4 h in the presence of concentrated H_2SO_4. The dimethyl ester of maleic acid thus obtained was distilled at 3 mm Hg (b.p. 330.2–331.1 K for the dimethyl ester). The purified maleic acid ester was sulfonated with an equimolecular amount of sodium hydrogen sulfite in H_2O at 373 K. A series of longer chain SDASs [dibutyl (SDBS), dihexyl (SDHS), and dioctyl (SDOS)], were prepared similarly, and were recrystallized in aqueous methanol. Sodium diheptylsulfosuccinate (SDHpS), sodium dinonylsulfosuccinate (SDNS), sodium didecylsulfosuccinate (SDDS), sodium diundecylsulfosuccinate (SDUS), and sodium didodecylsulfosuccinate (SDDoS) were prepared according to standard procedures [25, 26]. The amount of hydrated water in each crystalline sample was controlled by changing the growth rate of the crystals and was determined by Karl-Fisher titration (Kyoto Electric). The samples of SDAS(nH_2O) (n = hydration number) were classified into three sample systems: A series, SDBS($1H_2O$), SDHS($1H_2O$), SDHpS($1H_2O$) and SDOS($1H_2O$); B series, SDBS($2H_2O$), SDHS($2H_2O$, $3H_2O$), SDHpS($2H_2O$), SDOS($2H_2O$) and SDNS($2H_2O$), and C series, SDDS($1H_2O$), SDUS($1.3H_2O$) and SDDoS($1.5H_2O$). Identification of these samples was confirmed by ^1H and ^{13}C NMR spectra and elemental analysis (C, H and S%). All the reactants for preparation of SDMS, SDdMS and SDBS–SDOS were purchased from Wako Chemicals Co., and were purified before use. The reactants for preparation of SDHpS, SDNS, SDDS, SDUS, and SDDoS were purchased from Aldrich or Avocado Chemicals and were used without further purification.

Raman scattering spectral measurements

Raman spectra below 4000 cm^{-1} were obtained with a Nicolet 950 FT Raman spectrometer using a Nd: YAG laser (CVI) excitation wavelength of 1064 nm with a resolution of 4 cm^{-1} at room temperature (25 °C). The Raman spectra of the solid and solution samples were obtained from pressed solid samples in a capillary tube and from sample solutions put in a sealed capillary tube, respectively, with a laser power of 400 mW. Some of the samples for Raman scattering measurements were also excited by the 514.5 nm line of an Ar ion laser (NEC GLG-3200) and spectra were recorded on a JEOL JRS-400D Raman spectrometer. For measurements at low temperature (213 K), the samples were placed in a variable temperature capillary cell system (JEOL RS-VTC41).

Results and discussion

CH stretch modes of SDMS and SDdMS

The Raman scattering spectra of the crystalline SDdMS($1H_2O$) and SDMS($1H_2O$) samples are shown in Fig. 1A and B for the solid phase and aqueous solutions, respectively. The wavenumbers of the observed bands are listed in Table 1, along with tentative assignments.

For the Raman spectra of SDdMS($1H_2O$) in the crystalline state (Fig. 1A, spectrum a), the three Raman bands at 2938, 2966, and 2988 cm^{-1} obviously come from the CH stretch vibrational modes of the CH_2-CH segment. The first two bands may be assigned to the symmetric and asymmetric CH stretch modes of the CH_2 group, respectively, and the last band to the CH stretch mode of the methyne (>CH-) group.

In the Raman spectrum of SDMS (Fig. 1A, spectrum b), the band at 2938 cm^{-1} obviously comes from the symmetric stretch [$\nu_s(CH_2)$] vibrational mode for the CH_2 group of the CH_2-CH segment, and that at 2963 cm^{-1} is due to the asymmetric stretch mode [$\nu_{as}(CH_2)$] of the CH_2 group superimposed upon the

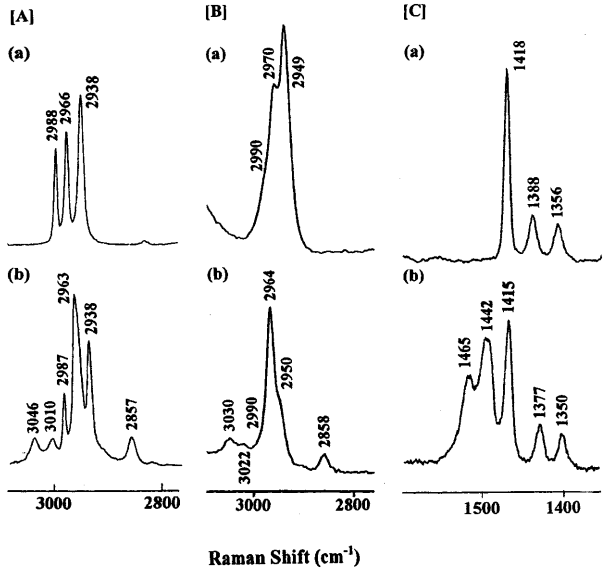

Fig. 1 **A** CH stretch Raman bands of solid sodium dideuteratedmethylsulfosuccinate (SDdMS) (*a*) and sodium dimethylsulfosuccinate (SDMS) (*b*) **B** CH stretch Raman bands of aqueous SDdMS (*a*), and SDMS (*b*) **C** CH_2 deformation Raman bands of solid SDdMS (*a*) and SDMS (*b*)

Table 1 CH and CD stretch Raman bands of sodium dimethylsulfosuccinate (SDMS) and sodium dideuterated-methylsulfosuccinate (SDdMS) in the solid state

SDMS			SDdMS			Assignment	
Solid		Aq. soln.	Solid		Aq. soln.	CH_3 or CD_3	CH_2-CH
Raman	IR	Raman	Raman	IR	Raman		
3046 w		3047 w				$\nu_{as}(CH_3)$	
		3022 w				$\nu_{as}(CH_3)$	
3010 w						$\nu_{as}(CH_3)$	
2987 m	2987 vw	2990 vw,sh	2988 m	2987 w	2990 w,sh		ν(CH)
2963 s	2964 w	2964 s	2966 m	2966 vw	2970 m	$\nu_s(CH_3)$	$\nu_{as}(CH_2)$
2938 m	2939 w	2950 sh	2938 m	2939 vw	2949 s		$\nu_s(CH_2)$
			2289 w	2288 vw			
			2263 w	2262 vw			
			2193 m	2196 vw	2193 m	$\nu_{as}(CD_3)$	
			2126 m	2126 vw	2131 m	$\nu_{as}(CD_3)$	
			2083 m	2081 vw	2087 vs	$\nu_s(CD_3)$	

symmetric CH stretch mode [$\nu_s(CH_3)$] of two CH_3 groups of the ester portions. The 2987 cm^{-1} band comes from the CH stretch mode of the methyne group. The two weak Raman bands at 3010 and 3046 cm^{-1} may be assigned to the asymmetric CH stretch modes [$\nu_{as}(CH_3)$] of the two methyl groups. For an SDMS molecule in the crystalline state, it has already been elucidated that the two methyl groups are in a nonequivalent environment [28]. Accordingly, an assignment of the CH stretch modes of the CH_3 groups which takes such an environmental difference into account is difficult; thus, for the CH_3 groups the assignment is tentative. The weak Raman band at 2857 cm^{-1} may come from the nonfundamental modes (combination modes) of the 1415 and 1442 cm^{-1} bands (Fig. 1C, spectra b).

In the Raman spectrum of SDMS, the intensities of the bands at 2938 and 2963 cm^{-1} may be influenced by Fermi resonance between the fundamental and nonfundamental modes, since combination modes, 1215 + 1728 (= 2943) and 1239 + 1728 (= 2967) cm^{-1}, are possible (spectra in the 1200–1800 cm^{-1} region not shown).

In a previous study [27], we elucidated the structure of the SDMS monohydrate in the crystalline state by single-crystal X-ray diffraction analysis. The result shows that although three rotational isomers (I, II and III) are possible for the conformations around the CH_2-CH single bond of the succinate skeleton (Fig. 2), isomer III is stabilized in the crystalline state. Therefore, in the Raman spectrum of SDMS, we may assume that the CH stretch bands coming from the CH_2-CH segment should reflect conformation III stabilized about the CH_2-CH single bond.

In the Raman spectrum of the aqueous SDdMS sample (Fig. 1B, spectrum a), it is evident that the bands at 2949, 2970, and 2990 cm^{-1} come from the CH_2-CH segment of a succinate skeleton. The first two bands may be assigned to the $\nu_s(CH_2)$ and $\nu_{as}(CH_2)$ modes of the CH_2 group, respectively. The last band may be due to the CH stretch mode of the methyne (CH) group.

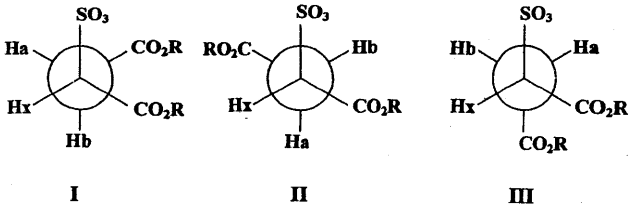

Fig. 2 Possible rotational isomers (I, II, and III) about the CH_2-CH single bond

In the Raman spectrum of the aqueous SDMS sample (Fig. 1B, spectrum b), the CH stretch modes of the CH_2-CH segment may be superimposed upon those of two CH_3 groups of the ester portions. The shoulder band at 2950 cm^{-1} corresponds well in frequency to the band at 2949 cm^{-1} and may be assigned to the $\nu_s(CH_2)$ mode. The strong Raman band at 2964 cm^{-1} is probably due to the $\nu_{as}(CH_2)$ mode superimposed upon the symmetric CH stretch mode of two CH_3 groups. The weak Raman bands at 3022 and 3030 cm^{-1} may be assigned to the $\nu_{as}(CH_3)$ mode of two CH_3 groups.

The weak band at 2858 cm^{-1} for the aqueous sample may be assigned to the nonfundamental modes (combination bands expected at 2860 cm^{-1}) of two CH_2 deformation modes (1417 and 1443 cm^{-1} for the solution sample, spectra not shown).

It should be noted that the $\nu_s(CH_2)$ and $\nu_{as}(CH_2)$ modes of the CH_2 group observed for the aqueous SDdMS and SDMS samples shift to a higher wavenumber [by 11–12 cm^{-1} for the $\nu_s(CH_2)$ mode by 4–6 cm^{-1} for the $\nu_{as}(CH_2)$ mode]. This shift may be caused by the coexistence of the rotational isomers I and II, as well as isomer III, in aqueous solution and by the change in the dielectric constants in the molecular environments upon resolution in water.

For solid SDdMS, five Raman bands at 2083, 2126, 2193, 2263, and 2289 cm^{-1} were observed in the CD stretch region. The last two bands disappeared for the

aqueous sample and only three bands at 2083, 2126, and 2193 cm^{-1} were observed (spectra not shown), indicating that the difference in the environment between the two CD_3 groups in the crystalline state may bring about the 2263 and 2289 cm^{-1} bands. Moreover, when considering the intensities of these CD stretch bands, the Fermi resonance should be taken into account, since the intensity pattern of the Raman spectrum becomes complicated due to the appearance of the nonfundamental modes [23].

The broad Raman bands at 1442 and 1465 cm^{-1}, which were observed for solid SDMS (Fig. 1C, spectrum b), disappeared in the spectrum of solid SDdMS (Fig. 1C, spectrum a). Therefore, these two bands may be assigned to symmetric and asymmetric deformation modes of the two methyl groups, respectively, and the nonequivalence of the two methyl groups [27] may broaden these bands.

CH stretch modes of the SDAS series with longer chains and the hydration effect

The Raman spectra of the A series in the CH stretch region are shown in Fig. 3. Since the bands at 2939–2943 and 2964–2968 cm^{-1}, which are observed in common, closely correspond to the 2938 and 2966 cm^{-1} bands, respectively, for crystalline SDdMS, we may assume that these bands make a large contribution to the symmetric and asymmetric CH stretch modes of the succinate CH_2 group, although the asymmetric CH stretch modes of the *n*-alkyl CH_3 groups may be superimposed upon these bands. The weak shoulder bands at about 2990 cm^{-1} may come from the succinate methyne (>CH-) group, since its band frequency corresponds well to the band frequency (2988 cm^{-1}) of the >CH- group of SDdMS. The Raman bands at 2847–2859, 2873–2877, and 2906–2914 cm^{-1} tend to increase in intensity with increasing chain length, and may thus be assigned to the CH stretch modes coming from the CH_2 groups of dialkyl chains.

The Raman spectra of the B series in the CH stretch region are shown in Fig. 4A. Obviously, the spectral features are different from those of the A series. For example, in the spectrum of the SDBS dihydrate, the 2943 and 2968 cm^{-1} bands, which were assigned to the succinate CH_2 portion of the monohydrate, have disappeared, and new Raman bands at 2888, 2918, and 2958 cm^{-1} are observed. Similar observations were also made for SDHpS($2H_2O$) and SDOS($2H_2O$). Therefore, for the dihydrate samples, it is difficult to assign exactly the CH stretch bands coming from the CH_2-CH segment. A possible explanation lies in the variation in

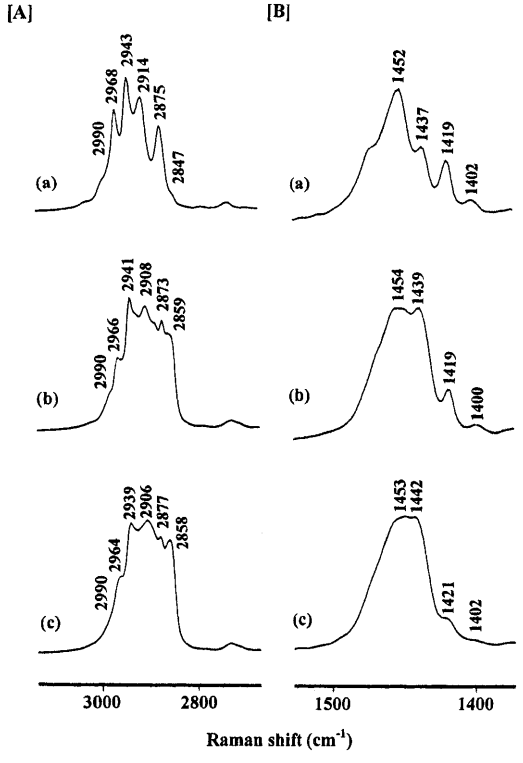

Fig. 3 **A** CH stretch and **B** CH_2 deformation Raman bands of the A series: (*a*) sodium dibutylsulfosuccinate (SDBS)($1H_2O$), (*b*) sodium diheptylsulfosuccinate (SDHpS)($1H_2O$), and (*c*) sodium dioctylsulfosuccinate (SDOS)($1H_2O$)

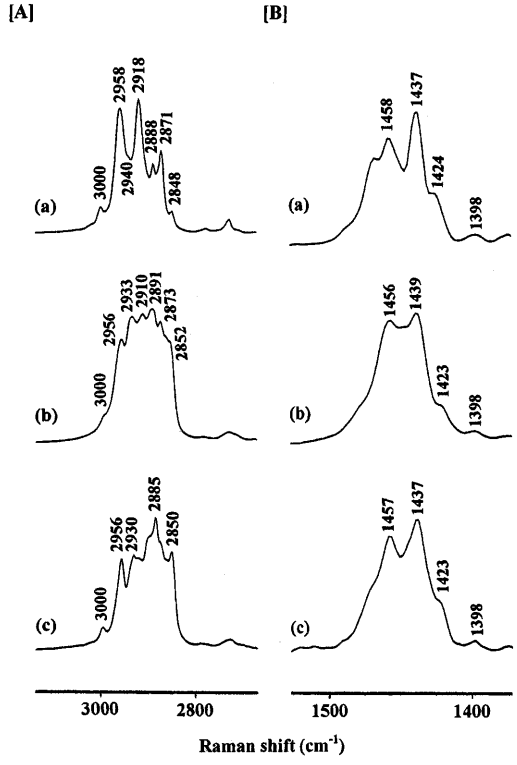

Fig. 4 **A** CH stretch and **B** CH_2 deformation Raman bands of the B series: (*a*) SDBS($2H_2O$) (*b*) SDHpS($2H_2O$), and (*c*) SDOS($2H_2O$)

the environment around the CH-CH_2 segment, due to the difference in packing of the hydrocarbon chains between the monohydrate and the dihydrate. However, the Raman bands at 2930–2940, 2956–2958, and 3000 cm^{-1}, observed in common for these dihydrate samples, may be tentatively assigned to the symmetric and asymmetric CH stretch modes of the succinate CH_2 group and the CH stretch mode of the methyne (> CH-) group, respectively.

Lucassen and Drew [28] reported that SDHpSs may be crystallized in two polymorphic modifications (a monohydrate and a dihydrate) and that for the dihydrate crystal the hydrocarbon chains have a zero angle of tilt with respect to the normal on the monolayer plane, while a possible structure for the monohydrate crystal deduced from the X-ray long spacings has an angle of tilt between the chains and the normal to the monolayer planes. That is, the dihydrate molecule tends to take up an untilted structure and the monohydrate molecules tend to take up a tilted structure, leading to the marked difference in packing of the hydrocarbon chains in their crystals.

Furthermore, in the untilted structure, there is a correct arrangement of enantiomers which depends upon formation of intermolecular hydrogen bonds with the two H_2O molecules. Conversely, in the tilted structure, there is less likelihood of a strict ordering of optical enantiomers because there are no hydrogen bonds in *a* direction which would lead to relaxation of the packing conditions in that direction and to disordering of the *n*-alkyl chains.

Crystal polymorphism, similar to that seen in the SDAS series, has already been confirmed for phospholipid systems, for example, for *n*-palmitoylgalactosylsphingosine [30], an untilted structure for the anhydrous crystal transforms into a tilted structure in the hydrated crystal. In dilauroylphosphatidyl ethanolamine [30], dehydration brings about conversion into a more stable form, implying that conversion into more stable forms involves either hydration or dehydration.

Thus, it may be assumed that the origin of the spectral changes in the CH stretch region is the difference in packing. For the dihydrate this spectral feature obviously reflects a strict ordering of the molecular arrangement, while that for the monohydrate reflects a disordered state.

The CH_2 deformation modes observed in the 1400–1500 cm^{-1} region, which are sensitive to molecular interactions [31, 32], are a useful monitor of the packing state of hydrocarbon chains in the gel or crystalline state. The Raman spectra of the A and B series in this region are shown in Figs. 3B and 4B. A marked difference in the spectral features (i.e., in the extent of splitting of this mode) is found between the A and B series: for the A series, the separations ($\Delta\nu$) between the Raman bands at 1437–1442 and 1452–1454 cm^{-1} are 15, 14, and 8 cm^{-1} for SDBS($1H_2O$), SDHpS($1H_2O$), and SDOS($1H_2O$) respectively and for the B series the $\Delta\nu$ values between the 1437–1439 and 1456–1458 cm^{-1} bands are 21, 17, and 20 cm^{-1} for SDBS($2H_2O$), SDHpS($2H_2O$), and SDOS($2H_2O$), respectively. The $\Delta\nu$ values for the dihydrate samples are larger than those for the monohydrate samples, showing that the hydrocarbon chains in the B series are more densely packed compared with those for the A series. Moreover, the spectral features of the A series in this region are generally broad, while those for the B series are relatively sharp, reflecting the difference in packing. This assumption is consistent with the results of single-crystal X-ray diffraction analysis of SDHpS($2H_2O$) and X-ray long spacings of SDHpS($1H_2O$) [28].

The Raman bands at 1400–1402 and 1419–1421 cm^{-1} for the A series and those at 1398 and 1423–1424 cm^{-1} for the B series may be assigned to the methyne (> CH-) and CH_2 deformation modes of the CH_2-CH segment, respectively.

Thus, for the SDBS–SDNS samples, we may conclude that the extent of hydration varies markedly with packing of the hydrocarbon chains in the crystalline state.

The Raman spectra of the C series in the CH stretch and CH_2 deformation regions are shown in Fig. 5. Generally, the Raman spectral features are found to be characteristic of the B series, since the Raman bands at 2848, 2883–2885, 2931–2934, and 2949–2951 cm^{-1}, observed in common with the B series, closely correspond to those at 2848–2850, 2884–2885, 2929–2930, and 2954–2956 cm^{-1}, respectively, for SDOS($2H_2O$) and SDNS($2H_2O$) (spectra not shown). The first two bands, which tend to increase in intensity with an increase in chain length, may be assigned to the CH_2 groups of the *n*-alkyl chains. In particular, the remarkably intensified bands at 2884–2885 cm^{-1} correspond well to the 2880 cm^{-1} band of a polymethylene chain [24], which takes up a trans zigzag structure, implying that these bands contain a great contribution from the extended form of the *n*-alkyl chains. The bands at 2993–2995 cm^{-1}, observed in common, may be assigned to the CH stretch mode of the methyne group.

It has been inferred that a significant part of the intensity of the Raman band at 2880 cm^{-1}, which can serve as an indicator of the phase transition of model membranes, is due to Fermi resonance between the in-phase CH_2 symmetric stretch fundamental and an overtone (or combination) of the CH_2 deformation modes [24]. For SDDS, SDUS, and SDDoS, we may expect that the combination bands between the 1414–1415 and 1437 cm^{-1} bands or between the 1456–1460 and 1437 cm^{-1} bands appear at 2851–2852 cm^{-1} or 2893–2897 cm^{-1}, respectively, resulting in an increased intensity of the 2848 cm^{-1} band or the 2883–2885 cm^{-1} band as a consequence of Fermi resonance. On the basis

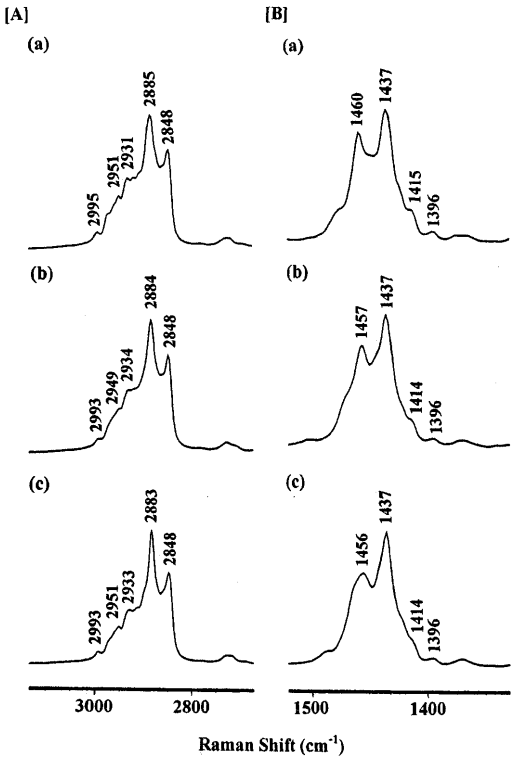

Fig. 5 **A** CH stretch and **B** CH_2 deformation Raman bands of the C series (*a*) sodium didecylsulfosuccinate (*SDDS*)(1H_2O), (*b*) sodium diundecylsulfosuccinate (*SDUS*)(1.3H_2O), and (*c*) sodium didodecylsulfosuccinate (*SDDoS*)(1.5H_2O)

of the results of our previous study on the CH stretch Raman bands of normal $C_{n-1}H_{2n-1}COOK$ (n = 3–18) [23], the intensities of the 2883–2885 cm^{-1} bands may be largely due to the intensity enhancement through Fermi resonance with the CH_2 symmetric stretch fundamental mode. This part of the intensity may be sensitive to changes in molecular state, resulting in the alteration of the intensity ratio, I(2883–2885 cm^{-1})/I(2848–2850 cm^{-1}), upon phase transition; therefore, for the long-chain SDAS–H_2O systems, this relative intensity ratio may be an indication of a phase transition.

The reason why the spectral features of the CH stretch modes for the C series are similar to those for the B series, rather than to those for the A series, may be explained as follows. An increase in hydrocarbon chain length probably induces the strictly ordered state of these long SDAS molecules upon close packing of the *n*-alkyl chains in the crystal lattice, which is not influenced by variation in the extent of hydration. In order to confirm this assumption, the long spacings for the C series were checked by X-ray powder patterns, as listed in Table 2, together with data for various SDASs which were obtained by Lucassen and Drew [28]. Both for untilted and tilted structures, it is evident that there exists a linear relationship between

Table 2 X-ray powder pattern long spacings for various sodium dialkylsulfosuccinate systems

n-alkyl group	Long spacing/Å	
	Untilted	Tilted
Hexyl	–	23.5[a]
Heptyl	32.6[a]	25.6[a]
Octyl	–	27.5[a]
Nonyl	38.4[a]	–
Decyl	41.1	–
Undecyl	43.9	–
Dodecyl	46.5	–
Hexadecyl	55.6[a]	–
Octadecyl	60.4[a]	–

[a] Long spacings reported by Lucassen and Drew [28]

long spacing and chain length, as reported by Lucassen and Drew [28]. The long spacings for the C series SDDS SDUS and SDDoS obviously fit a linear relationship for the untilted structure, showing that the molecules of the C series take up the untilted structure, which brings about the ordered state of the long *n*-alkyl chains.

Environmental change of alkyl chains upon phase transition and the CH stretch modes

Such a marked difference in the CH stretch band feature between the SDAS monohydrate and dihydrate may be used successfully to explore the environmental variation of the hydrocarbon chains caused by phase transition.

The Raman spectra of the coagel SDBS–H_2O systems with various SDBS concentrations are shown in Fig. 6A. For the coagel SDBS(5H_2O) sample (Fig. 6A, spectrum c), the CH stretch band feature is almost in accord with that of the SDBS(2H_2O) sample (Fig. 4A, spectrum a). In the spectrum of the coagel SDBS(28H_2O) sample, the characteristic 2940 cm^{-1} band of the SDBS monohydrate appeared, and with increasing concentration of SDBS in the original aqueous solution the intensity of this band increases until the spectral feature finally comes close to that of the SDBS monohydrate. The CH stretch band features of the coagel SDBS–H_2O samples, which were prepared from concentrated micellar solution (40 wt%) and from the lamellar samples (80 wt%), are generally very similar to that of the SDBS dihydrate, implying that the environment of the *n*-butyl chains in the coagel phase is similar to that in the dihydrate crystal.

The Raman spectra of the micellar solutions (20 and 40 wt%) and of the lamellar sample (80 wt%) of the SDBS–H_2O systems are shown in Fig. 6B. The CH stretch band feature of the lamellar sample is very

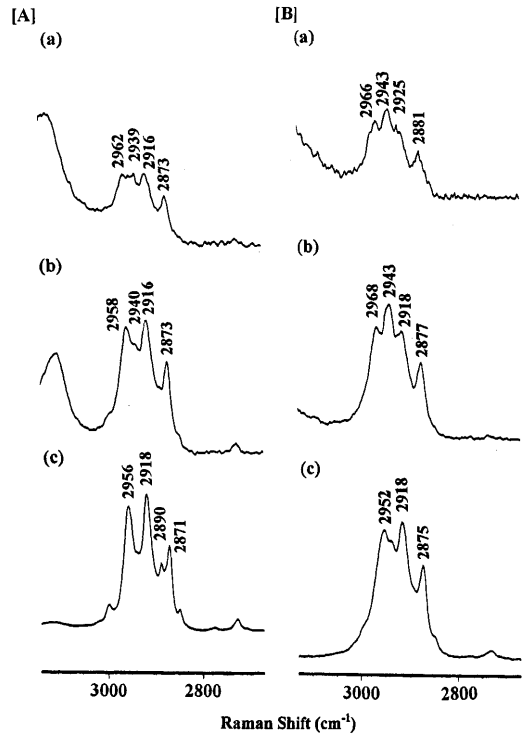

Fig. 6 Concentration dependence of CH stretch Raman bands for **A** the SDBS–H_2O system [(*a*) 20 wt%(74H_2O), (*b*) 40 wt%(28H_2O), (*c*) 80 wt%(5H_2O)] in the coagel state (213 K) and **B** the aqueous SDBS solutions [(*a*) 20 wt%, (*b*) 40 wt%, (*c*) 80 wt%]

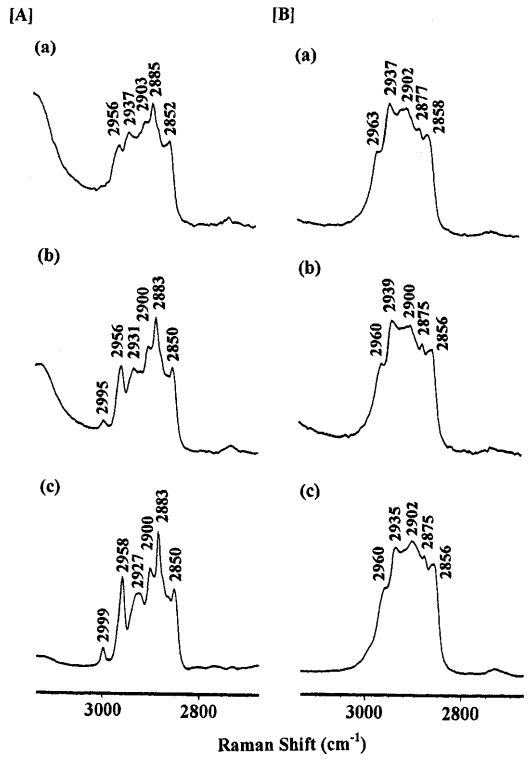

Fig. 7 Concentration dependence of CH stretch Raman bands for **A** the SDOS–H_2O system [(*a*) 20 wt%(99H_2O) (*b*) 30 wt%(58H_2O), (*c*) 60 wt%(16H_2O)] in the coagel state (213 K) and **B** aqueous SDOS solutions [(*a*) 20 wt% (*b*) 30 wt% (*c*) 60 wt%]

similar to that of the SDBS dihydrate, while those of the micellar solutions are similar to those of the monohydrate. The concentration dependence of the relative Raman peak height, I(2937–2941 cm^{-1})/I(2912–2917 cm^{-1}), in the CH stretch region was also examined for the SDBS–H_2O solutions above the critical micelle concentration. For the micellar solutions, the relative peak heights are almost constant, while formation of the lamellar structure brings about a marked decrease in the relative peak height, indicating that the extent of ordering of the hydrocarbon chains increases upon formation of the lamellar structure.

Similar observations have been made for the coagel, micellar, and lamellar samples of the SDHS–H_2O systems (spectra not shown).

The Raman spectra in the CH stretch region of the coagel SDOS–H_2O systems which were prepared from various concentrations of aqueous SDOS solutions, are shown in Fig. 7A. For the concentrated SDOS samples (20, 30, and 60 wt%) in the coagel state, the Raman bands at 2850–2852, 2883–2885, 2927–2937, and 2956–2958 cm^{-1} closely correspond to those at 2850, 2885, 2930, and 2959 cm^{-1}, respectively, for the SDOS dihydrate. Moreover, the spectral features are very similar to those of the dihydrate.

Conversely, for the concentrated aqueous SDOS solution (60 wt%) the Raman spectrum in the CH stretch region (Fig. 7B) is very similar to that of crystalline SDOS monohydrate. In fact, the bands at 2856–2858, 2875–2877, 2900–2902, 2935–2939, and 2960–2963 cm^{-1} correspond well with those at 2858, 2877, 2906, 2939, and 2964 cm^{-1}, respectively, for the monohydrate.

It is evident that the CH stretch band features of the coagel SDOS samples are of the dihydrate type, while those of concentrated aqueous SDOS samples are of the monohydrate type. Furthermore, it has been found that the split separations ($\Delta\nu$) between the CH_2 deformation bands at 1439–1441 and 1458 cm^{-1} for the those SDOS coagel samples are in the range 17–19 cm^{-1}, and are larger than those (13–15 cm^{-1}) for the concentrated aqueous sample solutions, reflecting the difference in packing of the *n*-octyl chains below the phase transitions.

The reason why the Raman spectral features of the CH stretch mode of the SDBS–, SDHS– and SDOS–H_2O systems in the micellar and lamellar states are analogous to those of the crystalline monohydrate and dihydrate samples may be related to the conformations of the hydrocarbon chains which are stabilized in

the aqueous solutions. This is discussed in detail below.

Longitudinal accordion-like vibrational modes of the SDAS series

Mizushima and Shimanouchi [33] and Schaufele [34] utilized the Raman scattering effect and found that for solid *n*-paraffins (C4–C16) at low temperature most of the polymethylene chains take up a fully extended geometry. This result was established from analysis of the longitudinal accordion-like vibrational modes which are characteristic of the polymethylene skeleton and whose frequencies are inversely proportional to the length of the polymethylene chain. Mizushima and Shimanouchi [33] found that the low-frequency vibrations of solid *n*-paraffins at low temperature could be fitted to a first-order approximation for the fundamental longitudinal frequency of a linear chain of identical harmonic oscillators,

$$\Delta v = (E/\rho)^{1/2}(2cd)^{-1}(m/n), \quad \text{when } m \gg n \ , \qquad (1)$$

where E is Young's elastic modulus, ρ is the density, c is the speed of light, d refers to the equilibrium distance between chain units, m is the vibrational order, and n is the number of chain units. This equation implies that the frequency is inversely proportional to the length (number of carbon atoms C_n), of the hydrocarbon chain.

For the Raman spectra of the B series in the 150–350 region (Fig. 8A), it is seen that the Raman bands, which are observed in common in the 200–300 cm^{-1} region, are shifted markedly to lower frequency with an increase in the *n*-alkyl chain length. Evidently, this variation in the spectral feature is characteristic of the longitudinal accordion-like vibrational modes of *n*-paraffins [33]. Figure 9 shows the linear relationship between the accordion band frequency and the reciprocal number of carbon atoms ($1/C_n$) for the SDAS series: only the band frequency of the accordion modes for SDBS does not fall on the line, a variation probably caused by coupling between the accordion modes of the short *n*-butyl chain and the deformation modes of the ester portions, which cannot be neglected in the short-chain compound. Therefore, the Raman bands observed at 295, 264, 255, 247, 239, and 228 cm^{-1} for SDBS($2H_2O$), SDHS($2H_2O$), SDHpS($2H_2O$), SDOS($2H_2O$), SDNS ($2H_2O$), and SDDS($1H_2O$) may be assigned to the longitudinal accordion-like bands of the *n*-butyl, *n*-hexyl, *n*-heptyl, *n*-octyl, *n*-nonyl, and *n*-decyl chains, respectively.

The longitudinal accordion-like vibrational bands of the A series have also been examined. Figure 8B shows the Raman spectral features of SDHS($1H_2O$) and SDHpS($1H_2O$) (as representatives) in the accordion mode region. For these monohydrates, the Raman

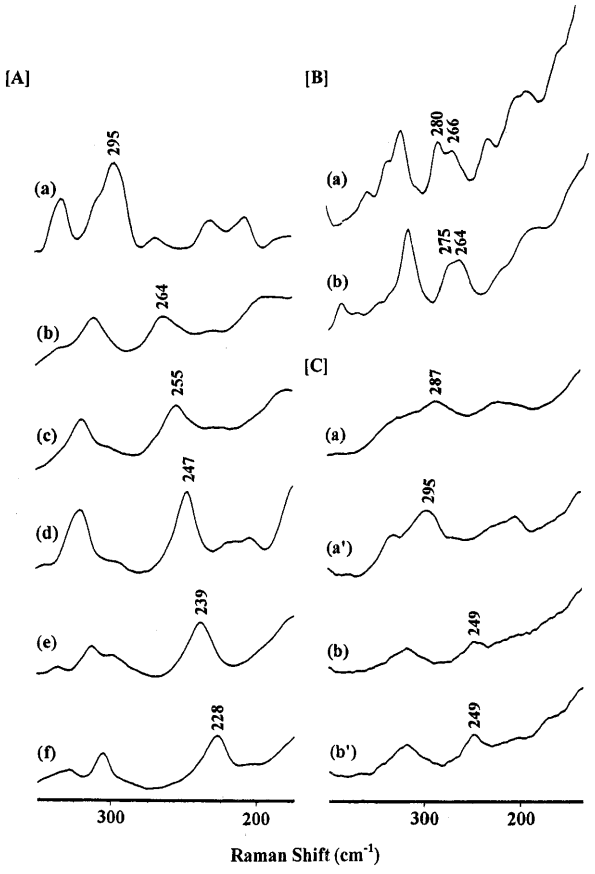

Fig. 8 Accordion-like vibrational bands of **A** the B and C series samples [(*a*) SDBS($2H_2O$), (*b*) sodium dihexylsulfosuccinate (SDHS) ($3H_2O$)*, (*c*) SDHpS($2H_2O$), (*d*) SDOS($2H_2O$), (*e*) SDDS($1H_2O$), and (*f*) SDUS($1.3H_2O$)] **B** the A series samples [(*a*) SDHS($1H_2O$) and (*b*) SDHpS($1H_2O$) and **C** the aqueous SDBS [(*a*) 70 wt%, (*a'*) 80 wt%] and SDOS [(*b*) 60 wt%, (*b'*) 90 wt%] solutions (*frozen samples)

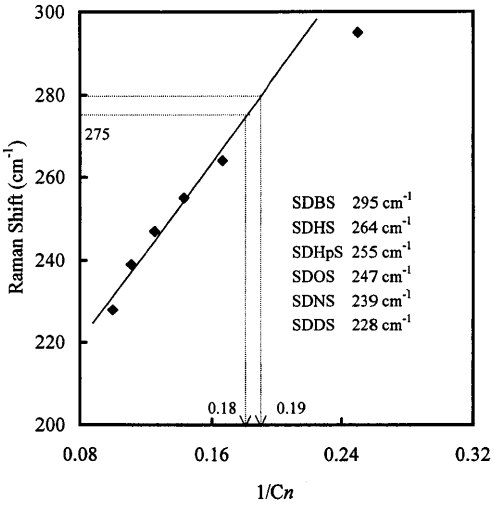

Fig. 9 Plots of the accordion band frequency against the $1/C_n$ value for the SDAS series. The inserted wavenumbers are the accordion band frequencies. The *insert* gives the corresponding accordion band wavenumbers

bands at 264–266 and 275–280 cm^{-1} have been observed in this region. The former bands correspond well to the accordion band at 264 cm^{-1} for SDHS($3H_2O$). It should be noted that the common bands, observed at 275–280 cm^{-1}, are positioned intermediate between the accordion band frequencies of SDBS and SDHS. Moreover, extrapolation (of the 275–280 cm^{-1} bands) of the linear accordion band frequency versus $1/C_n$ to the intercept provides an intercept value of 0.18–0.19 (Fig. 9, dotted lines), which corresponds to five carbon atoms. Therefore, we may assume that the 275–280 cm^{-1} bands come from the accordion mode of an extended $(CH_2)_5$ segment. It may be expected that for SDHS($1H_2O$), one of the two *n*-hexyl chains takes up the all-trans form and the other one takes up the TTTG form, and that for SDHpS($1H_2O$) one of two *n*-heptyl chains takes up the TTTTG form and the other one takes up the TTTGT form, as shown schematically in Fig. 10.

For SDOS($1H_2O$), two Raman bands at 256 and 280 cm^{-1} have been observed in the accordion mode region (spectra not shown). The frequency of the former band also corresponds well to that (255 cm^{-1}) of the accordion band of SDHpS($2H_2O$) and that of the latter band corresponds to that (280 cm^{-1}) expected for an extended *n*-pentyl segment. Thus, it may be assumed that for SDOS($1H_2O$), one of the two *n*-octyl chains of the segment corresponding to the *n*-heptyl chain is in the extended state, while for the other chain the portion corresponding to the *n*-pentyl chain is extended.

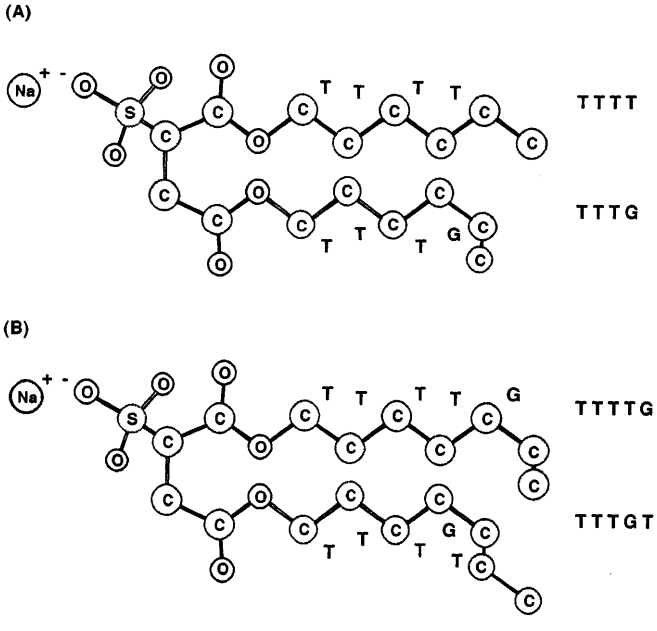

Fig. 10 Schematic presentation of the disordered skeleton of **A** SDHS($1H_2O$) and **B** SDHpS($1H_2O$); both samples in the solid state

Thus, such a splitting of the accordion mode observed in common for the SDAS monohydrates may indicate that the two *n*-alkyl chains are independent in disordered states. That is, the splitting behavior of the accordion mode provides ample evidence that the two *n*-alkyl chains of the SDAS monohydrates in the solid state are in the disordered state, supporting the reason why the CH stretch spectral features of the SDAS monohydrates are very similar to those for the aqueous SDAS samples. Indeed, it has already been elucidated by single-crystal X-ray diffraction analysis [27] that the methyl group of the β chain is in the disordered state even in a single crystal of sodium diethylsulfosuccinate. Furthermore, in the Raman spectra of the *n*-paraffins (*n*-butane–*n*-octane) in the liquid state, it has already been confirmed that such rotational isomers (TTTG, TTTTG, and TTTGT), containing one gauche form about the CH_2-CH_2 single bond close to the CH_3 terminal, are relatively stabilized as are the all-trans forms [34].

Moreover, for concentrated aqueous SDBS, SDHS, and SDOS solutions (lamellar phases), Raman bands have been found which correspond well to the frequencies of the accordion bands of these hydrocarbon chains. The accordion bands of the representative aqueous samples of SDBS and SDOS are shown in Fig. 8C. The presence of the accordion bands (the 287–295 cm^{-1} bands for SDBS and the 249 cm^{-1} band for SDOS) reveals that the *n*-alkyl chains are in the fully extended state in the lamellar phases; however, for the aqueous SDOS sample, there is an obvious shoulder band at about 280 cm^{-1}, in addition to the 249 cm^{-1} band (Fig. 8C, spectrum b). Therefore, a TTTG-type rotational isomer may coexist.

We have already reported that for surfactant molecules with relatively short chain length ($C_n \leq 8$) aggregation brings about predominant stabilization of the all-trans form [35, 36].

The similarity in the CH stretch band features between the concentrated aqueous SDAS sample and the crystalline SDAS systems, described previously, probably comes about from preferential stabilization of the all-trans form in the aggregated states, thereby promoting a closer packing and a more perpendicular arrangement of their *n*-alkyl chains.

Conclusion

In the SDAS series with relatively short chain length (C4–C8), the extent of hydration around the polar groups affects the manner of packing of the hydrocarbon chains, reflecting the Raman spectral pattern in the CH stretch region. In particular, it should be noted that for these series dihydration brings about an extended conformation of the *n*-alkyl chain, while monohydration makes the portion close to the terminal methyl groups

disordered. This result probably comes from the tilted structure in the molecular alignment and depends upon the extend of hydration.

However, for the SDAS series with longer chains (C10–C12) and close packing, the extent of hydration does not affect the CH stretch band feature.

Acknowledgements S.N. thanks the School of Chemistry, University of Bristol, for a Ph.D. scholarship.

References

1. Christopher DJ, Yarwood J, Belton PS, Hills BP (1992) J Colloid Interface Sci 152:465–472
2. Onori G, Santucci A (1993) J Phys Chem 97:5430–5434
3. Giammona G, Goffredi F, Liveri TV, Vassallo G (1992) J Colloid Interface Sci 154:411–415
4. Jain TK, Varshney M, Maitra A (1989) J Phys Chem 93:7409–7416
5. Blitz JP, Fulton JL, Smith RD (1989) Appl Spectrosc 43:812–816
6. D'Aprano A, Lizzio A, Liveri VT, Aliotta F, Vasi C, Migliardo P (1988) J Phys Chem 92:4436–4439
7. MacDonald H, Bedwell B, Gulari E (1986) Langmuir 2:704–708
8. Boicelli CA, Giomini M, Giuliani AM (1984) Appl Spectrosc 38:537–539
9. Faiman R, Lundström I, Fontell K (1977) Chem Phys Lipids 18:73–83
10. Maitra A, Jain TK (1987) Colloids Surf 28:19–27
11. Ayyagari XXuM, Tata M, John VT, McPherson GL (1993) J Phys Chem 97:11350–11353
12. Menassa P, Sandorfy C (1985) Can J Chem 63:3367–3370
13. Eastoe J, Fragneto G, Robinson BH, Towey TF, Keenen RK, Leng FJ (1992) J Chem Soc Faraday Trans 88:461–471
14. Moran PD, Bowmaker GA, Cooney RP, Bartlett JR, Woolfrey JL (1995) J Mater Chem 5:295–302
15. Moran PD, Bowmaker GA, Cooney RP (1995) Langmuir 11:738–743
16. Gaber BP, Peticolas WL (1977) Biochim Biophys Acta 465:260–274
17. Larsson K, Rand RP (1973) Biochim Biophys Acta 326:245–255
18. Bulkin BJ, Krishnamachari NJ (1972) J Am Chem Soc 94:1109–1112
19. Faiman R, Long DA (1975) J Raman Spectrosc 3:371–377
20. Mendelsohn R, Sunder S, Bernstein HJ (1976) Biochim Biophys Acta 419:563–569
21. Verma SP, Wallach DFH (1977) Biochim Biophys Res Commun 74:473–479
22. Schachtschneider JH, Snyder RG (1963) Spectrochim Acta 19:117–168
23. Okabayashi H, Kitagawa T (1978) J Phys Chem 82:1831–1836
24. Hattori N, Hara M, Okabayashi H, O'Connor CJ (1998) Colloid Polym Sci 277:306–317
25. Corkill JM, Goodman JF, Walker T (1965) Trans Faraday Soc 61:589–593
26. William EF, Woodberry NT, Dixon JK (1957) J Colloid Sci 12:452–459
27. Nagasoe Y, Hattori N, Masuda H, Okabayashi H, O'Connor CJ (1998) J Mol Struct 449:61–68
28. Lucassen J, Drew MGB (1987) J Chem Soc Faraday Trans l 83:3093–3106
29. Ruocco MJ, Atkinson D, Small DM, Skarjune RP, Oldfield E, Shipley GG (1981) Biochemistry 20:5957–5966
30. Seddon JM, Harlos K, Marsh D (1983) J Biol Chem 258:3850–3854
31. Snyder R, Schachtshneider JH (1963) Spectrochim Acta 19:85–116
32. Snyder RG (1967) J Chem Phys 47:1316–1360
33. Mizushima S, Shimanouchi T (1949) J Am Chem Soc 71:1320–1324
34. Schaufele RF (1968) J Chem Phys 49:4168–4175
35. Okabayashi H, Okuyama M, Kitagawa T (1975) Bull Chem Soc Jpn 48:2264–2269
36. Hattori N, Yoshida H, Okabayashi H, O'Connor CJ, Zana R (1998) Vib Spectrosc 18:83–90